The effect of thermal annealing on the properties of $Al_{1-x}Mn_x$ alloys grown by DC magnetron sputtering

Majda Mokhtari[1, 2], Abdel-Hamid Saker[1], Bouguera Bouzabata[1]

[1]Laboratory of Magnetism and Spectroscopy of Solids (LM2S), Physics department, Faculty of Science, Badji Mokhtar-Annaba University, 23200 Annaba, Algeria.
[2]Research Center in Industrial Technologies CRTI, P.O.Box 64, Cheraga 16104, Algiers, Algeria.
Corresponding author E-mail:: madjda.mokhtari@yahoo.fr, m.mokhtari@csc.dz

Abstract

In this paper, we report an investigation of structural, electrical and magnetic properties of the as-synthesized and annealed Al-Mn films. The $Al_{1-x}Mn_x$ thin films with Mn content ranging from 10.33 to 40.94 at.%, are prepared on cleaned microscope slide substrates using a direct current (DC) magnetron co-sputtering in a low-pressure argon atmosphere. Structural characterizations were analyzed using grazing incidence X-ray diffraction (XRD) on the as-deposited and heat treated at 773 °K samples. The electrical transport properties have been studied by Hall Effect measurements. The magnetic characteristics at room temperature were evaluated by a vibration sample magnetometer (VSM).

The X-ray diffraction patterns of the as-deposited Al-Mn films showed that increase in Mn for above ≈ 26 at. % transformed gradually the face-centered cubic (FCC) Al (Mn) solid solution into amorphous phase. After heat treatment XRD pattern revealed that all films have shown a crystal quality. The electrical and magnetic properties of Al-Mn films during annealing are significantly influenced by the transformations from amorphous to crystalline phases.

Keywords: ALUMINUM ALLOYS, MANGANESE, SPUTTERING, THIN FILMS, HEAT TREATMENT, STRUCTURAL, AMORPHOUS-CRYSTALLINE TRANSFORMATION

Introduction

Over the past few decades, aluminum and its alloys have been studied extensively, due to their industrial exploitation in high efficiency thin film for several electronic devices [1]. Among these alloys, the aluminum and manganese (Al-Mn) binary system presents a particular interest due to their suitable improved physical properties and it has already been used in a wide range of applications in nanotechnology, for example in novel NIS bolometers [2], Transition Edge Sensors (TES) microcalorimeters [3] and thin-film solid-state refrigerators [4]. Al-Mn films can currently be produced with various methods, like the rapid solidification (RS), melt quenching [5], electro-depositing [6], ion beam mixing [7] or physical vapor deposition (PVD) [8]. It is also known that during its synthesis intermetallic phases, icosahedral and decagonal quasicrystalline phases, as well as the amorphous phases might appear [9,10], as a result of the Mn addition that frustrates the FCC aluminum packing and induces atomic disorder in structural refinement by interdiffusion and subsequent phase transformations [11]. Currently, the amorphous-crystalline transformation can be obtained by different ways: (i) after annealing the amorphous film either in an inert atmosphere, or in an in situ electron microscope, (ii) or by the use of electron beam. In general, the post-annealing of amorphous thin films in order to

obtain specific crystalline structures is one of the methods by which intrinsic properties can potentially be developed to enable higher-performing devices. The transformation of amorphous Al-Mn alloys is usually observed above the temperature of 523 K (250 °C) [12], with the possible formation of metastable phases and the occurrence of a stable phase could depend on the kinds of germination nucleus in the amorphous film [13].

The main aim of this work was to explore the influence of Mn content on physical properties of $Al_{1-x}Mn_x$ alloys coatings deposited by direct current (DC) magnetron co-sputtering and annealed at 773 K.

Research Procedure

$Al_{1-x}Mn_x$ binary metallic thin films were grown on glass substrates using a DC magnetron sputtering method (Alcatel SCM 650 machine) at low temperature (floating temperature <400 K) from pure Al (99.99 % purity) and Mn (99.95% purity) targets. Suitable substrates such as glass slides were used for the study of the intrinsic behavior of the coatings. The growth conditions of Al-Mn films are listed in Table1.

The annealing treatment was done in vacuum at 773 K for 1h. The composition of the films was determined from energy dispersive X-ray spectroscopy (EDS) attached with MEB-FEI Phillips microscopy.

Table 1. Deposition conditions of Al-Mn thin films on glass slides

Distance target –substrate	80 (mm)
Pressure of work	55 (Pa)
Intensity target aluminum Intensity target manganese	3 (A) 0,5-1 (A)
Filming Intensity/ Tension	40/20 (A)/(V)

The as-deposited and annealed structures were examined by X-ray reflectivity (with $\lambda_{k\alpha}$(Co) and $\lambda_{k\alpha}$(Cu) radiations respectively). The electrical conductivity and Hall Effect characteristics were measured with the Van Der Pauw method. The magne- tic properties of Al-Mn layers were measured with Lakshor Instruments VSM at room temperature. The magnetic field (6 kOe) was applied parallel to the samples plane.

Results and Discussion

Microstructures of thin films

The compositions of the obtained films were determined using EDX, which revealed that the concentrations of Mn are from ≈ 10 to 41 atom per cent as Table 2 shows.

The XRD spectra of the as–synthesized Al-Mn samples with different Mn contents are displayed in Figure 1.

Table 2. Chemical compositions of the sputtered films (atomic % of magnesium)

Sample	1	2	3	4	5
at.% Mn	10.33	17.52	25.98	3231.72	40.94

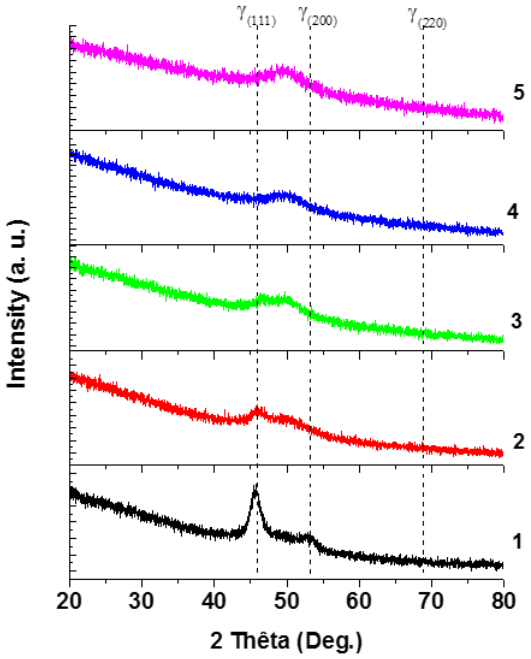

Figure 1.XRD patterns of the as-synthesized Al-Mn thin films ($\lambda_{k\alpha}$(Co) radiations), were 1: 10.33 at.%, 2: 17.52 at.%, 3: 25.98 at.%, 4: 31.72 at.%, 5: 40.94 at.%.

For the lower concentrations, between 10 and 26 atm. % of Mn, the as-synthesized coating X-ray patterns suggest that the face-centered cubic (FCC) Al-rich solid solution ($\gamma_{(hkl)}$) coexists with an amorphous phase. The observed shift of the most intense peak to higher angle, indicating a lower lattice parameter (refinement of grains), can be explained by the smaller atomic radius of manganese relatively to that of aluminum (0,137 nm for manganese against 0,143 nm for aluminum). For higher concentrations of Mn (32 and 41 atm.%), the diffraction peaks are broader and formed a broad hump visible at approximately 49° with no sharp peaks in the spectra. The films can therefore be regarded as amorphous structures [14].

Figure 2, shows the XRD patternsof the Al-Mn annealed samplesand the transformations from amorphous to crystalline phases are clearly seen. When the Mn content of the film is 10 at.%, with the (FCC) Al-rich solid solution ahomogeneous orthorhombic Al_6Mn solid solution of aluminum is formed . At 18 at. % of Mn, the solid solution Al(Mn) disappears and there is a growth of the Al_6Mn orthorhombic phase with the presence of the βMn cubic phase. But when the Mn content is increased to 26 and 32 at.%, the diffraction peaks of the XRD pat terns

can be identified due to Al_8Mn_5 (γ_2) and FCC-Al phases .

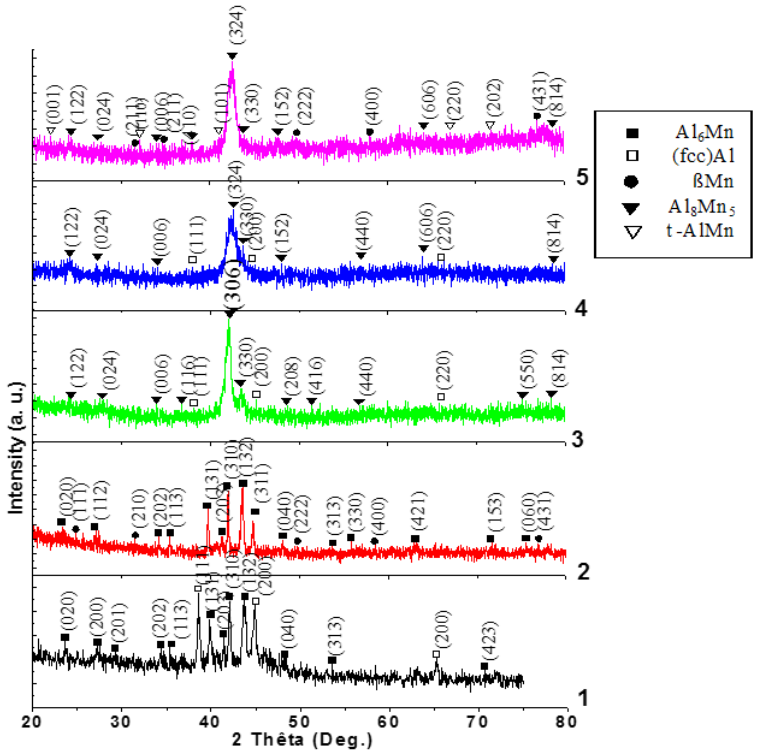

Figure 2. XRD patterns of annealed Al-Mn thin films ($\lambda_{k\alpha}$(Cu) radiations) were 1: 10.33 at.%, 2: 17.52 at.%, 3: 25.98 at.%, 4: 31.72 at.%, 5: 40.94 at.% .

At the highest content of Mn (41 at. %) , Al_8Mn_5(γ_2) and meta-stable ordered τ-AlMn phases are formed. It should noted that τ-AlMnis generally produced from a massive transformation of the ε phase that is usually observed at temperatures higher than 1073 K (as showed in the Al-Mn diagram phase) [15] Therefore,the formation of τ-AlMn depends on the annealing temperature and it decomposes into β-Mn and Al_8Mn_5(γ_2) after a lon period of isothermal annealing at high temperatures [13]. However, In the Al-Mn system, owe their hard magnetic properties to the τ-pahse with a composition range 42-49 at.% Al (51-52at.% Mn) [14]. The meta-stable τ-AlMn phase is not well defined in the Al-Mn phase diagram (figure 3), since it is formed in the range of 50-60 atm.% Mn [15, 16]. In our sample, its formation at lower concentration of Mn (41 at. %) might be related to co-sputtering process, a non-equilibrium technique.

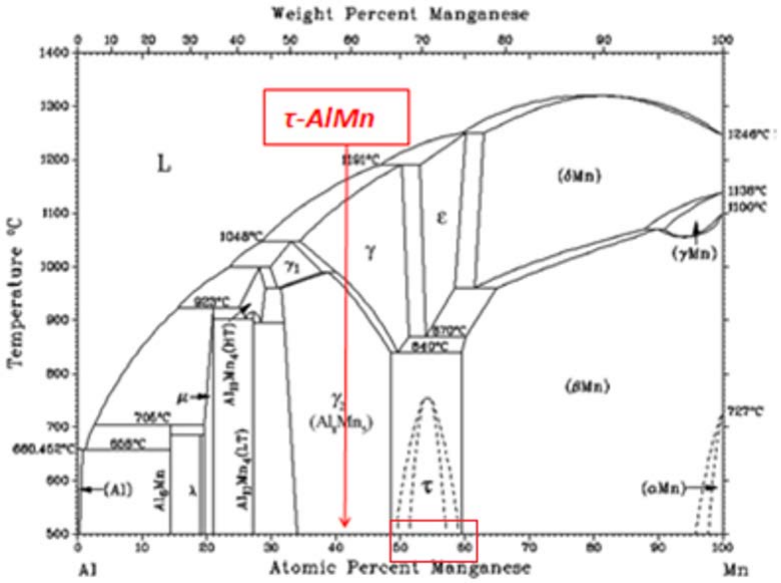

Figure 3. Al–Mn binary phase diagram [15], showing the τ-Al-Mn phase

Physical properties

Conducted by Hall Effect characteristics, comparative electrical studies of elaborated films; before and after annealing; (figure 4, 5 and 6) for the variations of the electrical conductivity (σ), the carrier concentration (n) and the electron mobility respectively showed that up to 18 at.% of Mn, for both films, it is observed a large decrease from the high value of the conductivity of pure Al ((σ (Al)= 3,7 10^{+5} $(\Omega.cm)^{-1}$) [17]) to about σ = 0 and 1.2 10^{+4} $(\Omega. cm)^{-1}$) respectively. This effect is due to the increase of amorphization up to a quasi-insulating behavior for the as-synthesized thin films, and the formation of the solid solution Al-rich at 10 at.% of Mn, followed by an almost complete crystallization at 26 at.% of Mn in the annealed thin films. Further concentration increasing of Mn does not change the conductivity, since both transformations are completed. Also, the microstructures of samples with the presences of a large concentration of defects in the as synthesized thin films that can be eliminated by annealing can explain the low metallic and the almost insulating behaviors in the two thin films. Likewise, was observed a decrease of the carrier concentration (n) in the as deposited films with increasing content of Mn is probably due to the increase rate of the formation of amorphous structure, inducing a higher structural disorder in grains boundaries, dislocations and precipitates, as well as the probable recombination of charge carriers. However, in the annealed Al-Mn films, the carrier concentration increases to a maximum value of n=7, 32 10^{+22} cm^{-3} at 18 at.% of Mn. A further increase in the concentration of Mn causes a decrease of (n) behavior close of t alloying effect of a conductor metal. On the other hand, the values of the electron mobility are very low and about the same for both films for low concentrations (up to of 26 at.% of Mn). For higher concentration of Mn (36 and 41 at.%), the electron mobility increases for the as-synthesized or amorphous films (about 1200 (cm^2/V.s)).

The resistivity of as-deposited Al-Mn thin films can be reduced because the grain growth is driven by reducing the grain boundary and surface energies, as well as after annealed by the formation of the precipitates of the Al alloy intermetallic compound [18]. The precipitates are potent nucleation sites for grains. Precipitation can also release compressive stress [18, 19]. The obtained results indicate that Al-Mn alloy films have better conductivity after heat treatment.

The magnetic characteristics ,obtained from the VSM results, indicate that all as-deposited and annealed films are not ferromagnetic at room temperature, except for the annealed sample with the relative concentration of 41 at.% of Mn , as figure 6 shows the depicting of magnetic hysteresis which is probably related to a magnetic properties of τ-AlMn.

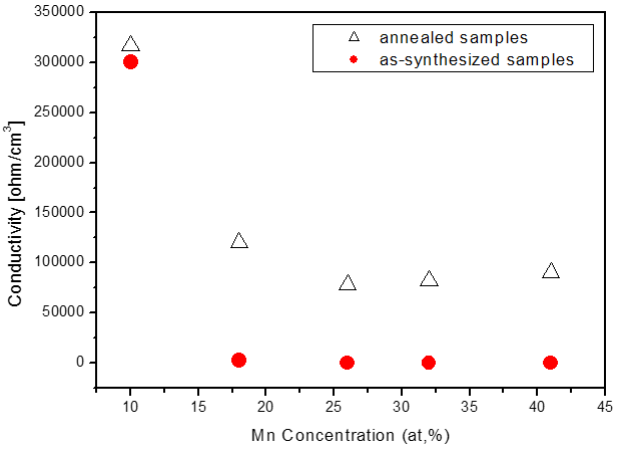

Figure 4. Variation of conductivity in Al-Mn thin films with Mn concentration

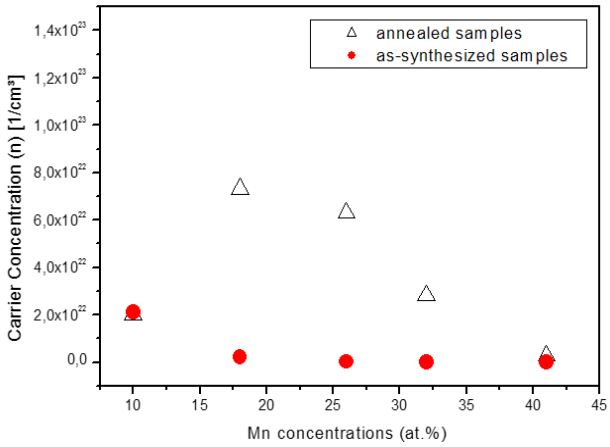

Figure 5. Variation of carrier concentration in Al-Mn thin films with Mn concentration

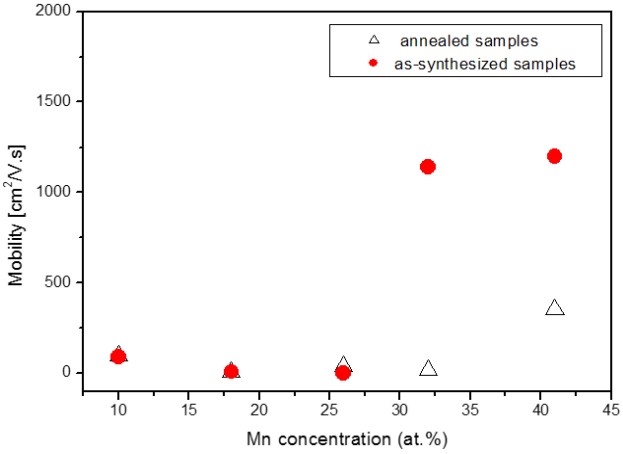

Figure 6. Variation of electron mobility in Al-Mn thin films with Mn concentration

The existence of τ-phase was confirmed in sample 5 as shown in figure 2.

Metastable τ-phase is an intermetallic compound

with a face center tetragonal (f.c.t) structure [14]. The magnetic characteristics for the annealed $Al_{59}Mn_{41}$ alloy are given by values: Hc = 81,05 Oe, and Ms (at H = 4000 Oe) = 1.63 10^{-4} emu/g . The small value of the highest magnetization Ms is probably due to the low amount of the τ phase embedded in all other formed phases.

However, the sigmoidal shape does not saturate at high applied magnetic field, with a round-off for over a magnetic field of 4 kOe. This decrease of magnetization at the approach of saturation can be explained by the change of the shape of magnetic domains from bands to bubbles, due to the possible thickness variations ending in a smaller mean magnetization [20, 21].

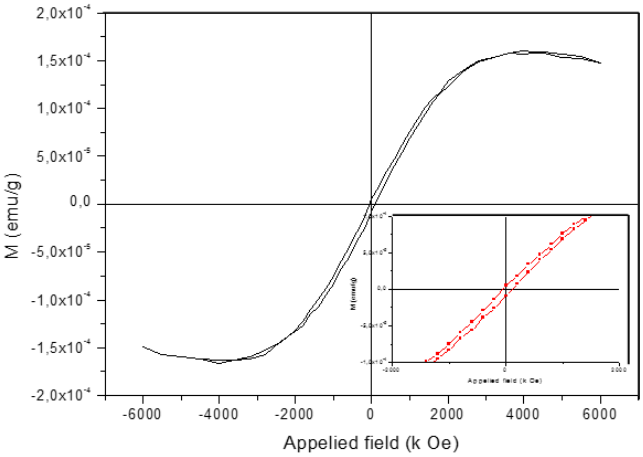

Figure 7. Hysteresis loop of 42% at. Mn after heat treatment

Conclusions

Aluminum-manganese non-equilibrium alloys have been prepared by DC magnetron sputtering in a low-pressure argon atmosphere from pure aluminum and manganese targets on glass substrates.

A structural study of as-deposited $Al_{1-x}Mn_x$ thin films obtained with x = 10.33, 17.52, 25.98, 31.72 and 40.94 at. % Mn reveals that increase in Mn for above ≈26 atom per cent will transform gradually the FCC-Al (Mn) solid solution into amorphous structure with probable local atomic arrangements.

The crystalline quality of Al-Mn thin films was improved by the post annealing in vacuum at 773 K, with the formation of several phases with varying degrees of deviation from equilibrium. The obtained phases after the amorphous-to-crystalline transition are as following: for 10 at. %of Mn, two phases are appearing being the orthorhombic-Al_6Mn and FCC-Al phases. For 18 at.% of Mn, the orthorhombic-Al_6Mn phase grows while βMn is appearing . For 26 and 32 at.% of Mn , the Al_8Mn_5 (γ_2) and FCC–Al phases are formed.

Finally, for 41 at.% of Mn , with the γ_2 phase , the ferromagnetic τ-AlMn phase is identified.

The electrical measurements of Al-Mn films are largely affected by the post annealing treatment due to the crystalline quality of structure. Moreover, room-temperature ferromagnetic is observed for annealed film with 41 at.% of Mn due to the presence of τ-AlMn ferromagnetic phase.

Acknowledgements

This work was supported by Laboratory of Magnetism and Spectroscopy of Solids (LM2S), Physics department, Faculty of Science, Badji Mokhtar-Annaba University, Algeria. The authors would like to thank all the persons having contribution in this research, especially for: Dr. S. BOUHOUCHE (UR-ASM-CRTI Annaba), Pr. N. BENSLIM (Annaba University), Dr. M. ZERGOUG (CRTI Algiers), Pr. M. GHERS (Annaba University), Pr. M.S. AIDA (Constantine University) Dr. A. SARI (CRNB-Ain-Oussera) and DR. A. BENSELHOUB (State Agrarian University, Ukraine).

References

1. Chen, C.H.;. Huang, H. E.; Materials Transactions, 2005, 46, 1413 - 1416.
2. Schmidt, D. R.; Lehnert, K. W.; Clark, A. M.; Duncan, W. D.; Irwin, K. D.; Miller, N.; Ullom, J. N.; *Appl. Phys. Lett.* 2005, 86(05),p. 3505.
3. S. W. Deiker, W. Doriese, G. C. Hilton, K. D. Irwin, W. H. Rippard, J. N. Ullom, L. R. Vale, S. T. Ruggiero, A. Williams and B. A. Young, *Appl. Phys. Lett.* 2004, 85,pp. 2137–2139.
4. DEVI, S.; BERGSTEN, T.; DELSING, P.; *Appl. Phys. Lett.* 2004, 84, pp. 3633–3635.
5. Sadoc, A.; Flank, A. M.; Lagarde, P.; *Physica* B 1989, 158, pp. 60-40.
6. ZHANG Lipeng, Xianjin YU, Yunhui DONG, Zengdian ZHAO, Enze CHEN, Hanbing LIANG, *Journal of Rare Earths* 2012,30 (3), pp. 278-282.
7. Kido, Y.; *Physics Research* B 1989, 37/38, pp. 696-700.
8. Ruggiero, S. T.; Williams, A.; Rippard, W. H.; Clark, A. M. Deiker, S. W.; Young, B. A.; Vale, L. R.; Ullom, J. N.; *Nucl. Instr. Methods in Phys. Res.* 2004, A520, pp. 274–276.
9. Du, Y.; Wang, J.; Zhao, J.; Schuster, J. C.; Weitzer, F.; Schmid-Fetzer, R.; Ohno, M.; Xu, H.; Liu, Z.; Shang, S.; Zhang, W.; *Journal of Materials Research* 2007, 98, pp. 855–871.
10. Koshlak H.V., Pavlenko A.M., Usenko B.O.,*Metallurgical and Mining Industry,* 2014, 2,

pp. 15-19.
11. Follstaedt, D.M.; Knapp, J.A.; *Materials science and engineering* 1987, 90, pp. 1–8.
12. Kaufman, M.J; Biancaniello, F.S; Kreider, K.G.; J. *Mater.Res*. 1988, 3, pp. 1342-48.
13. Reyes-Gasga, J.; Zou, B. S.; Mondragon-Galicia, G.; JosYacamfin, M.; *Thin Solid Films* 1993, 230, pp. 108-114.
14. AnuragChaturvedi, RumanaYaqub, Ian Baker, Metal 2014, 4(1), pp. 20-27.
15. T.B Massaski. Binary Alloy Phase Diagrams. Materials Park (OH): TMS; 1990.
16. Vlasova, N.I.; Kandaurova, G.S.; Shut Ya. S.;.Bykhanova, N. N. ;*Phys. Met. Metall.* 1981, 51, pp. 212-218.
17. Chin T.S; Magn, J.; Magn. Mater. 2000, 209, 75-79.18 Onishi, T.; Iwamura, E. ; Takagi, K.; *Thin Solid Films* 1999, 340, pp. 306–316
18. Hyde, K. B.; Norman, A. F. ;Prangnell, P. B; *Acta Mater.* 2001, 49, pp. 1327–1337.
19. Robert W. Messler, Jr.,T*he Essence of Materials for Engineers*,Jones and Bartlett Learning, 2011.
20. Kono, H.J.; J. *Phys. Soc. Jpn.* 1958, 13, pp. 1444-1451.
21. T. Godecke, W. Koster, Z. *Metallkd*. 1971, 62(10), pp. 727-732.

Effect of inoculation by molybdenum and nickel on hardening phenomenon and wear behavior of high manganese steel

Hichem Maouche [1,2], Ali Hadji [1], Khadija Bouhamla [1,2]

[1]Foundry Laboratory, Faculty of Engineering, Department of Metallurgy and Materials Engineering, Badji Mokhtar Annaba University, P.O. Box 12, Annaba 23000, ALGERIA.
[2] Research Centre in Industrial Technologies CRTI, P.O.Box 64 Cheraga 16014 Algiers, ALGERIA.
E-mail: hichemcsc@gmail.com, h.maouche@csc.dz

Abstract
Manganese steel demonstrates a great rate of work hardening during service, together with good toughness, leads to its widespread use in the heart switching crossings of railways, excavators, mineral crushing equipment and other severe mechanical environments. The specification for the standard steel has 10–14% manganese and 1.0–1.4% carbon, although modern variants often include chromium as well. Its structure is fully austenitic in the normal quenched condition. In this study we focus on the influence of inoculation by molybdenum and nickel and molybdenum-nickel on the surface hardening or the hardened part and wear resistance of the manganese steel. The melting of this steel is carried out in an industrial electric furnace. The transformation of austenite during operation, thus determines the steel operating lifetime, the rate transformation of austenite to martensite can introduce a compromise between ductility and wear resistance of the steel to support large efforts without breaking. The purpose of this